

Analysis and Evaluation of Topological and Application Characteristics of Unreliable Mobile Wireless Ad-hoc Network

Serdar Cabuk, Nipoon Malhotra, Longbi Lin, Saurabh Bagchi, Ness Shroff
School of Electrical and Computer Engineering, Purdue University
465 Northwestern Avenue, West Lafayette, IN 47907.
Phone: 765-494-3362. Fax: 765-494-2706.
Email: {scabuk, nmalhot, llin, sbagchi, shroff}@purdue.edu

Abstract

This paper presents a study of topological characteristics of mobile wireless ad-hoc networks. The characteristics studied are connectivity, coverage, and diameter. Knowledge of topological characteristics of a network aids in the design and performance prediction of network protocols. This paper introduces intelligent goal-directed mobility algorithms for achieving desired topological characteristics. A simulation-based study shows that to achieve low, medium and high network QoS defined in terms of combined requirements of the three metrics, the network needs respectively 8, 16, and 40 nodes. If nodes can fail, the requirements increase to 8, 36 and 60 nodes respectively. We present a theoretical derivation of the improvement due to the mobility models and the sufficient condition for 100% connectivity and coverage. Next, we show the effect of improved topological characteristics in enhancing QoS of an application level protocol, namely, a location determination protocol called Hop-Terrain. The study shows that the error in location estimation is reduced by up to 68% with goal-directed mobility.

Keywords: *ad-hoc mobile wireless network, topological characteristics, goal-directed mobility algorithms, simulation study, node failures.*

1. Introduction

A mobile ad hoc network is an autonomous system of mobile hosts connected by wireless RF links. There is no static infrastructure such as base stations. If two hosts are not within radio range, all message communication between them must pass through intermediate hosts which double as routers. Sensor networks are a particular class of wireless ad hoc networks in which the nodes have micro-electro-mechanical (MEMS) components, including sensors, actuators and RF communication components. Sensor nodes are randomly dispersed over the area of interest and are capable of short-range RF communication (≈ 100 ft) and contain signal processing engines to manage the communication protocols and for data

processing. The individual nodes have a limited processing capacity, but are capable of supporting distributed applications through coordinated effort in a network that can include hundreds or even thousands of nodes. Sensor nodes are typically battery-powered and since replacing batteries is often very difficult, reducing energy consumption is an important design consideration for sensor networks. Since the transmission range of a node is proportional to the square root or fourth root of the transmitting power, the range of a sensor node is constrained in most deployments.

In many applications of wireless ad hoc networks, the hosts are mobile which complicates analysis of network characteristics because the network topology constantly changes. The analysis is made more challenging by the fact that the sensor nodes are likely to be more failure-prone than traditional wired, larger scale devices and will typically be deployed for extended periods of time.

The network characteristics considered in the study are connectivity, coverage, and diameter. These characterize the network's utility in running useful higher layer protocols. Complete connectivity in the network implies communication is possible between any two pairs of nodes. Coverage indicates the percentage of the sensor field that can be sensed by at least one node and therefore, properties of the area can be known. Diameter is the maximum number of hops between any two nodes and the product of diameter and per hop latency serves as the upper bound on the communication delay in the network. The paper presents goal directed mobility algorithms whose objective is to improve the measure of each individual characteristic with a tolerable degradation in the others, which are specifiable in the mobility determination step. The underlying model is that the sensor nodes are carried by actuators which can be controlled remotely, according to the algorithms proposed here, in order to place the nodes in desired topologies.

There have been theoretical studies that have looked at a single parameter (connectivity in [7]) or two parameters (connectivity and degree in [8]) in a static wireless environment. However, these studies have not considered the effect of mobility (or done so for asymptotic cases of number of nodes), and transient and permanent failures on

the network characteristics. Also, goal-directed mobility patterns that can be employed to improve the network characteristics have not been studied in such environments. There exists a volume of work on the low-level energy-aware routing protocols in ad-hoc wireless and sensor networks. In our work, we are not concerned with the routing protocol in use and assume the most appropriate routing protocol is in place in the system.

In the paper, we present a theoretical derivation of the sufficient condition for connectivity and coverage in a two-dimensional grid of nodes which can move and can fail. A previous study [11] had considered these properties in the case of random node placements and a second study [12] had studied them in the case of stationary nodes with failure probabilities but neither considered the network properties with goal-directed mobility and failures. A previous study had looked at only network connectivity with mobility in a two-dimensional ad-hoc wireless network [4]. We believe this is the first study to evaluate a combination of network characteristics and investigate the effect of transient and permanent host failures on them. We also consider the effect of the network characteristics on an important application for sensor networks, namely, location determination. The workload relies on a fraction of the nodes, called *anchor nodes*, having *a priori* knowledge of their location and diffusing the knowledge through several rounds of a distributed protocol. The application specific metric that is studied is the percentage error in the location determination and it is shown that the goal-directed mobility algorithms reduce the error by up to 68%.

The rest of the paper is organized as follows. Section 2 presents the measures of interest in the study, the failure model, the goal-directed mobility algorithms, and the workload. Section 3 presents the theoretical proofs for the mobility algorithms and the derivation of the sufficient condition for 100% connectivity and coverage with node mobility and node failures. Section 4 presents the simulation model. Section 5 provides results and Section 6 concludes the paper.

2. Design of Study: System Model, Protocols and Parameters

2.1. System Model

We consider a sensor network model for the ad-hoc network. Each node has a limited transmission range which is constant for the node when it is functional. The nodes have the capability of motion in any direction in the two-dimensional grid space. There are constraints on the maximum speed of motion of the nodes. A node can respond to control messages dictating direction and velocity of motion. This allows the system to perform

intelligent motion of the sensor nodes which is used in the study to achieve desired network topologies. Since the transmission range of each node is limited, communication between two nodes in the network may have to go through multiple hops. DSR is used as the routing protocol in the study. The sensor nodes transmit in omni-directional mode and therefore the graph representing the network is undirected with an edge signifying the two nodes have a distance less than their transmission range.

2.2. Parameters for Network Characteristics

The most obvious and well-studied network property of relevance to a networked application is *connectivity*. A desired network characteristic is that the communication graph representing the network be strongly connected, i.e., for every pair of nodes there exists a path between them. We define the connectivity of the network as follows. Consider that the graph has several strongly connected components creating mutually disjoint clusters of connected components in the network. Let the strongly connected components of the graph be ordered in decreasing order of size. The ordered list is C_1, C_2, \dots, C_k and the respective sizes are G_1, G_2, \dots, G_k . The first definition of connectivity we propose is

$$CONNECTIVITY = G_1/n$$

By this definition, only the largest connected component is relevant to the network. An alternate definition is to consider the fraction of connected components which have greater than a threshold number of nodes in them. In this study, we do not have a well-defined threshold and therefore, we use the first definition of connectivity in this paper.

The *diameter* of the network is the diameter of the communication graph and is defined as the number of hops in the longest path between any two nodes in the graph. Knowing the diameter of the network and the per-hop delay allows one to place an upper bound on the communication delay in the network which may be of importance for the soft real-time nature of several sensor applications.

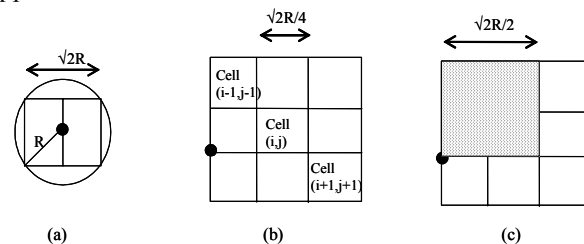


Figure 1. Coverage estimation

The third parameter of interest is *coverage* which is defined as the percentage of the total sensor field that is covered by at least one node. A point being covered implies the point is in the sensing radius of at least one node in the system. Coverage is an important metric for several application scenarios of sensor networks, such as surveillance and target tracking. In this study, we do not make the common assumption that transmission range and sensing range are identical. The transmission radius is represented by r and the sensing radius by R . We calculate a lower bound estimate on the coverage since the exact analysis with a rectangular field and circular transmission region is computationally expensive and not suitable for use in multiple iterative steps of a simulation. A square that is inscribed in the circle of radius R is completely covered by the node at the center of the circle. Such a square, shown in Figure 1(a) has sides of length $\sqrt{2} * R$ and is called the *square_sense_region (SSR)* for the node. To estimate coverage of the sensor field, it is divided into square cells of side $\sqrt{2} * R / 4$ each (Figure 1(b)). Any such cell is covered if there is a node in either that cell or in any of the eight neighboring cells. To understand this, consider a node placed at the grid point shown in Figure 1(c). It completely covers a square region of side $\sqrt{2} * R / 2$ which is one quadrant of its square transmission region from (a). Therefore the entire cell (i, j) is covered by this node. The coverage of the network is given by the fraction of cells covered by the total number of cells which is L^2 / SSR^2 .

2.3. Failure Model

In the study we consider only node failures and not link failures. It is of course understood that link failures may also be possible due to several factors including mobility, noise and interference in wireless channels. However, we propose to study its effect in a separate study. The node failures can be either permanent or transient. In the failed state, crash failure semantics is exhibited. The permanent node failures may be due to the exhaustion of the power source on the node, or a permanent physical damage to the node. The transient node failures are caused either by the motion of the node to a region where it is unable to communicate with any other node, or motion of another node in its transmission range that causes interference. The time between failures and time to recovery for transient failures follow exponential distributions.

2.4. Goal-Driven Mobility Algorithms

The algorithm for motion has the objective of meeting the requirements of coverage, connectivity, and diameter *simultaneously*. The connectivity and coverage requirements bound the allowable values from below

(e.g., connectivity must be greater than 90%), while the diameter requirement bounds it from above. The algorithm runs iteratively and at each step, it chooses one of two possible mobility algorithms depending upon which metric has been satisfied and which needs to be improved.

The first mobility model is meant to decrease diameter and is called the *Mean Shift Clustering (MSC)* algorithm. Consider a naïve motion (called *Baseline MSC*) of moving a node to the centroid of all its neighbors which are up to k hops away, called *k-and-less-neighbors*. The sum of the distances of a node from its k -and-less-neighbors is minimized by the motion. This has the potential of decreasing the diameter of the network if the longest path was from the node being moved to one of its k -and-less-neighbors. However, the result of the motion would be that all the nodes would collapse to a single point and would lead to negligible coverage. The model we use for decreasing diameter is suggested by this naïve model, but preserves coverage. Instead of moving a node to the centroid, it is moved a fraction of the distance and then the move is evaluated using an evaluation function. The evaluation function, henceforth called a *local evaluation function (LEF)* is given by:

$$LEF = w1.Sum\ of\ distances\ from\ k - and - less\ neighbors - w2.Distance\ from\ centroid$$

If the LEF gives a negative value, the node is not moved. Intuitively, for high coverage, the nodes should be spread out and the first term should be higher. For low diameter, the second term should be smaller. Depending on which of the parameters has already been satisfied, the values of $w1$ and $w2$ can be adjusted. For normalization, instead of absolute values, relative changes are considered from the previous value.

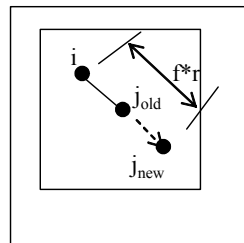


Figure 2. Node motion by algorithm SNA designed to increase coverage and connectivity

The second mobility model is meant to increase connectivity and coverage and is called the *Shift Neighbors Away (SNA)* algorithm. The algorithm can be thought of as sweeping through the sensor field, once from left to right starting at the top and next from right to left starting at the bottom pushing the nodes away from each other without disconnecting two immediate neighbors. In the sweep from left to right, when a node i is considered, all the nodes in the fourth quadrant of its SSR are pushed away from the center of node i . A neighbor can be pushed a maximum of r distance away without disconnection. However, to avoid the situation of many nodes squished at

the bottom of the field, the push is a fraction f of r . The fraction f is a decreasing function of the number of nodes. The working of the algorithm is shown schematically for two nodes i and j in Figure 2. Node i is the current node in the algorithm and node j is the neighbor that is to be pushed away. A similar process is followed when the sweep is done from the right to the left starting at the bottom.

The intelligent motion algorithm executes either MSC followed by SNA, or just SNA depending on whether diameter constraints have been satisfied or not. After the execution, a *global evaluation function (GEF)* is evaluated to decide whether to preserve the motion or roll it back. GEF incorporates all three parameters and is higher for better topologies. It is given by:

$$GEF = W1.Connectivity + W2.Coverage - W3.Diameter$$

The obtained parameter values are normalized with respect to the desired values. Also, if a desired value for a parameter has been reached, its impact is de-emphasized by setting the weight for that parameter to zero. If a move is rolled back, a random perturbation of the nodes is employed followed by MSC-SNA or SNA singly. Note that rolling back is an artifice of the simulation and does not correspond to nodes retracing their path. The function can be calculated *a priori* to the execution of motion and the decision to execute the movement or not taken based on the GEF value. Also, the global state of the network cannot be known by any one node and therefore the GEF computation has to be approximated by considering a portion of the sensor field that is in a node's proximity.

2.5. Workload: Robust Location Determination

The workload selected for the study is a robust location determination algorithm for wireless sensor networks. The algorithm is a two-step one consisting of the Hop-TERRAIN algorithm [5] that runs in the startup phase and an iterative Refinement algorithm [6] that runs after the startup. In the network, a few of the nodes, called *anchor nodes*, have location information, through special hardware at the node, such as a GSM receiver. This information is *diffused* to other nodes through multiple transmissions. The estimate of location using a single anchor is not reliable because of impreciseness in measurements, such as using received signal strength to determine distance. The protocol reduces the error margin by collecting relative positions with respect to several anchors and solving a set of redundant linear equations. On termination of the algorithm, each node has an estimate of its position with respect to a global coordinate scheme.

Location determination of wireless nodes is an important problem since the information gathered by a node often needs to be interpreted based on the location of

the node. The problem becomes challenging when only a fraction of the nodes can act as anchor nodes. Also, the range estimation between neighbor nodes is subject to errors because of errors in physical measurements, such as the received signal strength, and impreciseness in the mapping of the physical measurements to the range estimation. The protocol being considered here is robust with respect to both these constraints – few anchor nodes and errors in range estimation between neighboring nodes. The error in the final position estimate made by the non-anchor nodes is the QoS metric of the protocol. It is a function of the number of one hop neighbors that have received the diffusion, called *neighbor connectivity*, and the number of anchor nodes from which the diffusion has been received, called *anchor connectivity*.

3. Theoretical Analysis

3.1. Theoretical Analysis of MSC and SNA

The MSC algorithm is based on the mean shift clustering approach [13]. Baseline MSC collapses the mobile nodes into clusters and it can be shown that all nodes in a cluster converge to a single point. Moreover, the rate of convergence of this algorithm is along the gradient of the distribution of nodes and is thus along the path of steepest ascent. This makes the algorithm an ideal choice for reducing a mobile network's diameter.

Let $x \in S$ be the position of a node. The algorithm proceeds by iteratively calculating the sample mean over a window of nodes in the neighborhood. The position for the node to move to in the next motion step is given by

$$m(x) = \frac{\sum_{s \in S} K(s-x) \cdot s}{\sum_{s \in S} K(s-x)}$$

The function $K(x)$ is a weighting kernel and decides the size of the window in space which is used to compute the next location and the weights assigned to each point in the window. For the MSC algorithm, we choose a flat kernel of the form

$$K(p) = \begin{cases} 1, & \text{if } |p| \leq \lambda \\ 0, & \text{if } |p| > \lambda \end{cases}$$

In words, the position is determined equally by all nodes which are up to λ distance away and not at all by more distant nodes. In [13], it has been shown that if λ is set to the diameter of the network (called global mean shift), then all the nodes in S converge to a single point. The algorithm gives the steepest ascent with a varying step size in the magnitude of the gradient. Mathematically, the rate of convergence is given by at least $\frac{\partial m(S)}{\partial S}$. If every

node is iteratively moved to the centroid of all the nodes in the field, then the diameter converges to zero. It is also

shown that if only k-hop neighbors are considered (constrained mean shift), then the nodes converge to multiple clusters with the rate of convergence being equivalent to the one above, in the individual cluster.

This work forms the motivation for the Baseline MSC algorithm with $\lambda = 2r_{tx}$, the transmission radius. However, the coverage is zero for global mean shift and is upper bounded by number of clusters times the sensing radius of a node in the constrained mean shift algorithm. In most practical deployments of a sensor network, coverage of the field is an important criterion. Therefore we modify Baseline MSC to take the decrease in coverage into account and therefore, oppose the clustering.

In order to analyze the SNA algorithm, we first consider an infinite plane and place the n nodes in this plane in s super-cells, where each super-cell consists of the block of nine cells considered in Figure 1(b) and has dimension of $\frac{3\sqrt{2}r}{4}$. For the rest of this discussion, we

will refer to these super-cells simply as cells. Our claim is that for this ideal case of the infinite plane, SNA converges with a coverage increase of factor $(n-s)/s$, where s is the number of initially covered cells.

Lemma 1: After SNA converges, there is at least one node in each initially covered cell.

Proof: From the definition of SNA, if a node is the last node in a cell, it does not leave the cell. This proves that the cells which are initially covered stay covered, between the initial placement and the converged network.

Lemma 2: After SNA converges, there is at most one node in every cell.

Proof: From the definition of SNA, the “earliest” node is chosen in a cell and all other nodes are displaced by $f \times r$. The value of f has to be chosen appropriately such that all but the “earliest” node is displaced from the cell. The

diagonal of the cell is $\sqrt{2} \cdot \frac{3\sqrt{2}R}{4} = \frac{3R}{2}$ and therefore

$f \times r > \frac{3R}{2}$, i.e. $f > \frac{2r}{3R} = \frac{2}{3} \kappa$. Also, the nodes are

displaced to cell(s) which is(are) going to be subsequently visited by SNA. By “earliest”, we mean the node which is visited first in a sweep of SNA, e.g., for the left to right horizontal sweep, it is the node with the smallest X-coordinate in a cell.

Theorem 1: After SNA converges, the coverage increases by a factor $(n-s)/s$.

Proof: It follows from Lemmas 1 & 2 that after SNA converges, there exist n cells with n nodes in them as compared to the initial topology which had the n nodes distributed among s cells. The increase in number of covered cells is $(n-s)$ and the relative increase is $(n-s)/s$.

Next, we relax the infinite plane assumption and assume instead there is a large enough finite plane such that there is room for diffusion of all the nodes.

Theorem 2: After SNA converges, the coverage is improved over the Random Way Point (RWP) model of motion.

Proof: Since we have large enough space for diffusion of all the nodes, it is guaranteed by Lemmas 1 & 2 that we will have exactly one node in each cell after SNA converges. Hence, $P(\text{Greater than one node in a cell}) = 0$

Consider random placement of n nodes in an $L \times L$ plane. $P(\# \text{nodes in a cell} > 1) = 1 - [P(\# \text{nodes in a cell} = 0) + P(\# \text{nodes in a cell} = 1)]$. Consider a one-dimensional flattening of the L^2 cells and the problem can be mapped to allocating a mix of L^2-1 bars and n balls in $n+L^2-1$ slots since drawing L^2-1 bars gives L^2 boxes and encloses the n balls. The number of ways in which this can be done is $C_{L^2-1}^{n+L^2-1} = C_n^{n+L^2-1}$. The first term is then

given by $\frac{C_n^{n+L^2-2}}{C_{L^2-1}^{n+L^2-1}} = \frac{C_{L^2-2}^{n+L^2-2}}{C_{L^2-1}^{n+L^2-1}}$ and the second term by

$\frac{C_{n+1}^{n+L^2-3}}{C_{L^2-1}^{n+L^2-1}} = \frac{C_{L^2-2}^{n+L^2-3}}{C_{L^2-1}^{n+L^2-1}}$. Thus,

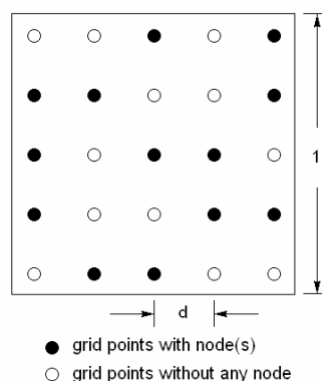
$$P(>1 \text{ node in a cell}) = 1 - \left[\frac{C_{L^2-2}^{n+L^2-2}}{C_{L^2-1}^{n+L^2-1}} + \frac{C_{L^2-2}^{n+L^2-3}}{C_{L^2-1}^{n+L^2-1}} \right]$$

$$= 1 - \frac{(L^2-1)(2n+L^2-2)}{(n+L^2-1)(n+L^2-2)} \geq 0 = 1 - \frac{(1-1/L^2)(2n/L^2+1-2/L^2)}{(n/L^2+1-1/L^2)(n/L^2+1-2/L^2)} \rightarrow 0, \text{ as } L \rightarrow \infty$$

The above equations show that there is a finite non-zero probability of more than one node in a cell which adversely impacts the coverage. Next, when RWP motion is applied to this random placement, it has been shown in [14] that the nodes cluster towards the center of the sensor field. This will affect the coverage even further. Thus, SNA achieves better coverage than RWP.

3.2. Theoretical Analysis of Connectivity and Coverage

3.2.1. System Model. Consider a sensor network arranged



in a grid over a unit square area. A node can only stay at one of the grid points. There are altogether n such grid points, which we will later refer to as *positions* of nodes. The distance between the two adjacent positions is therefore $d = 1/\sqrt{n}$, as shown in the following figure.

In this model, nodes can only stay at grid points. As we

later let n tend to infinity, nodes can be at positions arbitrarily close to any given point within the unit square area.

Initially there is a node at each position in the network. Movements can only occur at $t = NT$, where $N = 1, 2, \dots$, and T is the fixed duration for the time slot. At $t = NT$, each node randomly chooses a destination position k (it can also choose to remain stationary), and reaches position k immediately. The next movement is chosen at $t = (N+1)T$.

As a way of removing the edge effect, we extend the grid to the entire two-dimensional plane, keeping the separation of $1/\sqrt{n}$ between two adjacent positions unchanged. There is also a node at each grid point outside the unit square initially. Nodes can move across the boundary of the unit square. We number all the positions with $k = 1, 2, \dots$, and the node initially at position k is named node k . Let K be the set of all nodes, including the ones outside the unit square. It is worth noting that there are other ways to remove the edge effect, besides the assumptions made above. For example, we can assume that, when a node leaves the boundary from one side of square, it enters the other side of the square in a symmetric fashion. Alternatively, we can assume the grid is deployed on a large sphere. But doing so, we need to slightly modify the other assumptions, but the same analytical results will still hold.

Define $P_{kl}^N = \text{P}(\text{node } k \text{ appears at position } l \text{ at time } t = NT)$

In order to derive the sufficient condition, we need the following two assumptions:

(A1) The selection of the destination relative to current position is of independent and identical distribution among all nodes.

(A2) $\lim_{N \rightarrow \infty} P_{kl}^N = 0, \forall k \in K$

The second assumption means that after the system runs long enough, the probability for any given node to appear in any given position is vanishingly small. One example of such a mobility model is the standard two-dimensional random walk, where a node goes to one of its four adjacent neighbor positions with equal probability. It is clear that in our model we can also allow nodes to go to a faraway position in one time slot, and allow different probability for a node to go in different directions. Nodes can fail independently and the failures are transient. At any time t , the probability for a node to be in the state of failure is $q(n)$.

3.2.2. The Sufficient Conditions for Coverage and Connectivity. We now calculate the probability that there is no node in a given position l . Note that this probability does not depend on the l . Let

$$P_{open}^N = \text{Pr}(\text{There is no node at position } l \text{ at time } t = NT).$$

Since node movements are independent,

$$P_{open}^N = \text{Pr}(\bigcap_k \{\text{node } k \text{ is not at position } l \text{ at time } t = NT\}) = \prod_k (1 - P_{kl}^N)$$

Let j be the position symmetric to position k with respect to position l . Since node movements are i.i.d, the probability for node k to appear at position l is the same as the probability for node l to appear at position j , or $P_{kl}^N = P_{lj}^N$. And the j 's exhaust all the possible positions that node l can go to. It follows that:

$$P_{open}^N = \prod_k (1 - P_{kl}^N) = \prod_j (1 - P_{lj}^N) = \exp(\sum_j \log(1 - P_{lj}^N)) \leq \exp(\sum_j (-P_{lj}^N)) = e^{-1}.$$

The above equation uses the fact that $\log(1 - x) \leq -x, \forall x \in [0, 1]$, and $\sum_j P_{lj}^N = 1, \forall l$.

Define the probability that there is no node at a given position in the steady state as $P_{open} = \lim_{N \rightarrow \infty} P_{open}^N$.

From (A), it is clear that $P_{open} \leq e^{-1}$. In fact, using assumption (A2), we can show $\forall \epsilon > 0, P_{open} \geq e^{-(1+\epsilon)}$ for large enough N . Since ϵ is arbitrary, we have $P_{open} = e^{-1}$.

That is, the probability that there is no node at a position tends to e^{-1} , after the system runs for a long enough time.

Since the sensor nodes are unreliable, even if there are nodes in a given position, there may still be no active nodes in that position. Recall that the probability for a node to be in the state of failure is $q(n)$. Let

$$P_{inactive} = \text{Pr}(\text{There is no active node at a given position}),$$

$$P_i = \text{Pr}(\text{There are } i \text{ nodes at a given position}).$$

Then

$$\begin{aligned} P_{inactive} &= P_{open} + \sum_i P_i \text{Pr}(\text{all } i \text{ nodes fail}) = P_{open} + \sum_i P_i q^i(n) \\ &\leq P_{open} + \sum_i P_i q(n) = P_{open} + (1 - P_{open})q(n) = e^{-1} + (1 - e^{-1})q(n) \end{aligned}$$

We now map our scenario to the stationary unreliable sensor grid case in [12]. In the stationary case, n nodes are arranged in a grid over a unit square and nodes fail independently and with a certain probability $\hat{q}(n)$. In our case, although the nodes are moving, the positions, or grid points, remain stationary. With this observation in mind, we assume there is one *virtual* node in each grid point over the unit square. Those virtual nodes are stationary and fail with probability $P_{inactive}$. In other words, we take $P_{inactive}$, the probability that there is no active node at a given position, to be the $\hat{q}(n)$ in [12].

However, the difference between our virtual-node model and the original stationary model is that the failures between the virtual nodes are no longer independent; they all depend on node movements. If a position is covered by a node k , the virtual node at this position has some chance to be active. Meanwhile, the same node k will not be at

any other position, so the virtual nodes at those positions have slightly less chance to be active.

Note that we have the following relationship:
 $P(\text{No node at } k \text{ or } l) = P(\text{No node at } k | \text{No node at } l) \cdot P(\text{No node at } l)$
 $\leq P(\text{No node at } k) \cdot P(\text{No node at } l)$

Using the above equation in the proof of the sufficient conditions in [12], we are able to show that

$$P(\text{Network is 100\% connected and covered}) \geq 1 - \left(\frac{1}{\alpha r(n)}\right)^2 (e^{-1} + (1 - e^{-1})q(n))^{\pi \beta^2 r^2(n)n},$$

for any $\alpha > 0$ and $\beta > 0$ such that $\alpha + 2\beta = 1$. And the sufficient condition for asymptotic connectivity and coverage is given by

$$\lim_{n \rightarrow \infty} \frac{n(1 - q(n))r^2(n)}{\log(n)} > \frac{e - 4}{e - 1} \frac{4}{\pi}.$$

The above sufficient condition for asymptotic connectivity with coverage is close to the one in the stationary case. This implies that the impact on connectivity and coverage due to the mobility in our sensor network is not significant.

4. Simulation Model

The network simulator *ns-2* is used as the simulation environment. The nodes are initially placed on the grid points and move in discrete steps from one grid point to another according to the goal-directed motion algorithms described in Section 2.4. The initial placement of the nodes is not uniform random contrary to most simulation studies. We simulate a practical scenario in which the sensor nodes is in two equal-sized clusters at the top left and at the bottom right of the sensor field from which they diffuse out using the mobility algorithms. Consider for example a sensor network being used to monitor the chemical composition of the air in a building in an emergency situation and nodes deployed initially close to the entrances.

First, we describe the simulation method for the failure free case. The simulation is started with user inputs for the desired values and the minimum tolerable levels of the output metrics. For a study focusing on one of the metrics, the desired values and the minimum levels for the others are kept low (or high, depending on what is good for the metric). Initially, a small number of nodes (5) are placed in the field. The simulation is run for a fixed time with the given number of nodes, called *epoch interval*, and iterated a fixed number of times, called *epoch iterations*. The epoch interval is conservatively taken as five times the mean of the exponential distribution which gives the duration of uniform motion of a node. The reasoning is that the metrics should be measured when the nodes are paused in between their motion steps. Taking a factor of 5 gives a 99% probability that all nodes have stopped

moving. A node motion at any of the steps is rejected if it causes the minimum levels of any of the metrics to be violated. If the constraints are met within epoch iterations, then the simulation is terminated, otherwise an additional node is inserted.

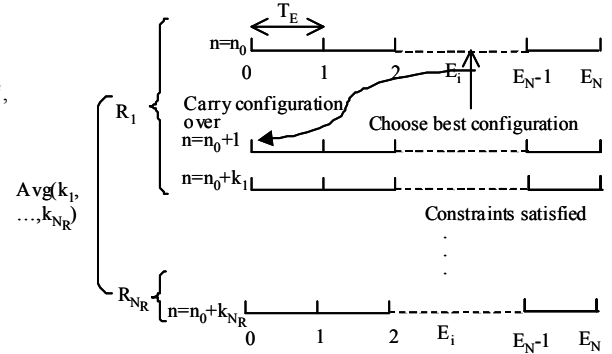


Figure 3. Simulation methodology. A total of R_{N_R} runs with E_N epoch iterations in each run, each epoch of length T_E . Node addition uses the best configuration from previous case.

For inserting the additional node, the best configuration from the previous run is maintained and a node is added at a grid point in the sensor field which was not covered. The best value, rather than the average, in the epoch iterations is taken. The rationale is that if there is a particular configuration with the given number of nodes that can achieve the level, that particular configuration can be accepted. The node addition algorithm is a simplified one since only coverage is considered. A more comprehensive one should add the node depending on which metric threshold was not met. Since an exhaustive node placement is not possible, the number of trials is used as a heuristic to conclude the impossibility of satisfying the constraints with a given number of nodes. A schematic showing the simulation method is represented in Figure 3.

Table 1. Simulation parameters

Parameter	Value
Sensor field dimension	500 m X 500 m (1 m grid)
Initial placement regions	Two bands: (0,0) – (70,70). (430,430) – (500,500).
Node transmission range	125 m
Mean epoch length (T_E)	200 ms
Mean Time to Failure	200 ms
Mean Time to Repair	20 ms
Permanent:Transient failures	10:90
Number of runs (N_r)	5
Epoch iterations (E_N)	40

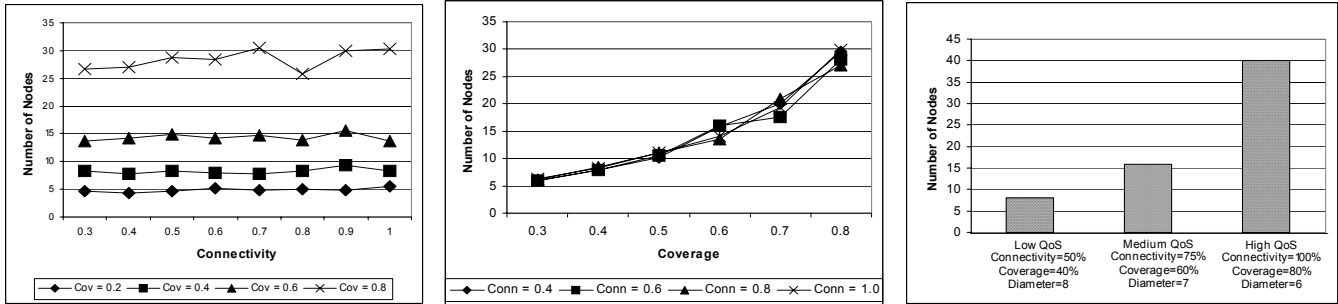


Figure 4. (a) Variation of number of nodes required for desired connectivity; (b) Variation of number of nodes required for desired coverage; (c) Number of nodes required for achieving low, medium and high QoS levels

5. Results

5.1. Failure Free Study

In the first set of experiments, we investigate the question of how many nodes are needed to meet a threshold measure of the output metric or a desired QoS combining all the metrics. Our model is a sufficient upper bound to this number for various levels of QoS. Figure 4 shows the behavior of the network with different combinations of connectivity and coverage requirements where each result is an average of ten such runs with diameter kept at a low QoS value of eight. The number of nodes needed looks to be exponential with the coverage requirement (Figure 4(b)) while not significantly affected by the connectivity requirement. This is reasonable since, for instance, having two connected nodes in a network of two nodes gives 100% connectivity, while coverage of the area is highly dependent on the number of nodes and their intelligent placement and movement. The observed fluctuations in both graphs are as a result of random components in the model - additional node placement, and random movement of the isolated nodes. However, multiple runs smooth out most of the fluctuations.

Next, we combine the requirements for the different metrics and look at a set of requirements for meeting the aggregate QoS levels (Figure 4(c)). We define three QoS levels for this purpose and label them Low QoS (Connectivity=50%, Coverage=40%, Diameter=8), Medium QoS (Connectivity=75%, Coverage=60%, Diameter=7), and High QoS (Connectivity=100%, Coverage=80%, Diameter=6). While only 8 and 17 nodes are required for Low and Medium levels respectively, the High QoS requires as many as 41 nodes. This is expected because of the exponential behavior of these metrics at the high-end of the spectrum when almost full coverage and connectivity are desired.

5.2. Node Failure Study

The second set of experiments includes the node failure cases where transient or permanent node failures can occur as described in Section 2.3. The expected behavior of the system response is increased requirement for the number of nodes for the same QoS requirements with more fluctuations due to the exponential model we are using in modeling the failures. The number of epoch iterations is 20 and each epoch interval is 23 seconds, giving a network lifetime of 460 seconds. The results in this section are dependent on the network lifetime since that determines the absolute number of failures.

In the first of these experiments, we find the number of nodes required to satisfy three different QoS levels for different failure rates. MTTF=INF gives the failure-free case and the corresponding result is taken from Figure 4(c). From Figure 5, we see that the effect of transient node failures is significant when the MTTF is small (50 or 100). The MTTF of 200 approximates the error free case. Moreover, it can be seen that for the low QoS, there is no significant difference between the failure-free and the failure case. This is because with small number of nodes, it is easier to come up with *chance* configurations which satisfy the constraints.

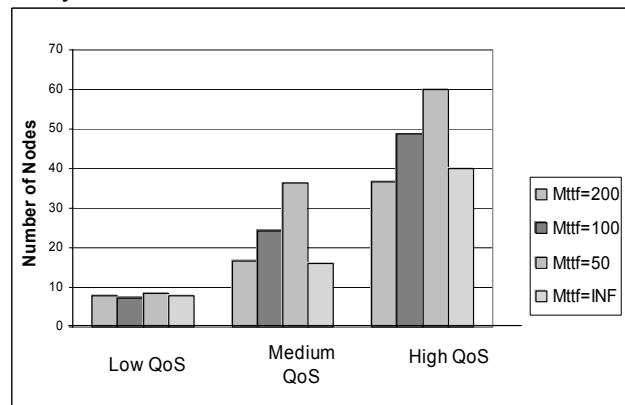


Figure 5. Number of nodes for supporting low, medium and high QoS levels for different error rates.

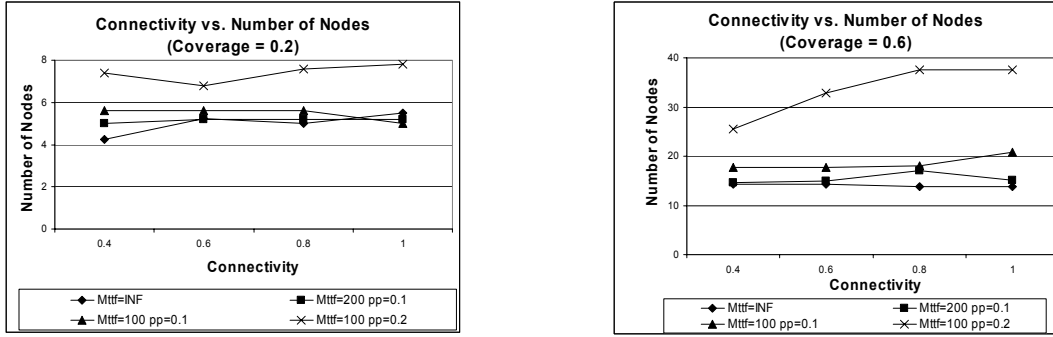


Figure 6. Variation of number of nodes required for desired connectivity for coverage of 0.2 and 0.8 respectively (diameter = 8).

In the next set of experiments we look at the individual output metrics with the node failures. In the first of this set, we look for the change in connectivity with different levels of coverage, MTTF and permanent to transient node failure ratio. It is observed in Figure 6 that MTTF does not have much impact in this scenario. This is again due to the fact that the MTTF values are quite high compared to the simulation time, and the number of nodes is not large. Consequently, the absolute numbers of failures in the different cases are close. In contrast, when the proportion of permanent failures is doubled to 20%, the effect is significant and number of nodes required is almost doubled as well. Although this is a connectivity graph, this effect mainly comes from the coverage component which degrades drastically when nodes are lost due to permanent failures. Finally, the effect of coverage metric shown in Figure 7 is similar to the failure-free model. Increasing the coverage requirement results in significant increase in number of nodes, while being relatively insensitive to connectivity.

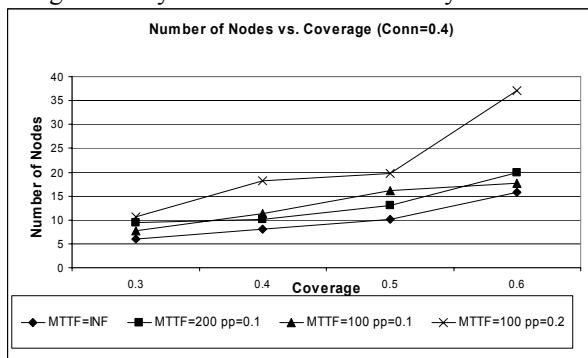


Figure 7. Variation of number of nodes required for desired coverage (Connectivity = 0.4)

The improvements are shown in Table 2. Importantly, the relative improvement increases with increasing number of nodes. This is explained by the observation that

5.3. Workload Based Study

In this set of experiments, we evaluate the impact of the goal-driven mobility models on the error in location estimation from the Hop-TERRAIN and Refinement application. The error is measured for the topologies arrived at using goal-directed mobility and compared with that from topologies arrived at by using the RWP model. The error in Hop-TERRAIN is a function of the average number of neighbors of a node that have calculated their own locations relative to those of at least three anchor nodes. The count of such neighbors for a node is henceforth called *Neighbor Connectivity*. In the first experiment, we vary the number of sensor nodes, keeping the proportion of anchor nodes constant at 5%. We let the goal-driven motion achieve a coverage of 80% with a diameter of six and measure the neighbor connectivity. Similarly, the neighbor connectivity is measured after moving the nodes for the same amount of simulation time using RWP. Given neighbor connectivity, the error is looked up from [9].

Table 2. Improvement in error in location estimation due to goal-directed motion with varying number of nodes

n	Random Motion		Goal-directed Motion (80% coverage, diameter=6)		Improvement (%)
	NC	ξ (%)	NC	ξ (%)	
30	5	22	11	12	45.5
40	6	20	14	8.5	57.5
50	7	18	17	7	61.1

n : Number of nodes; NC: Neighbor connectivity; ξ : Error

the goal-directed motion is further capable of optimizing the topological characteristics with a larger number of

nodes to place while RWP being random in nature cannot benefit from this.

Next, we show that the extent of improvement of the application QoS can be controlled for a given number of nodes by varying the topological characteristics that the goal-directed motion achieves. The results with the number of nodes kept constant at 30 are shown in Table 3. Expectedly, the improvement is most marked when the mobility algorithms achieve low diameter. However, a network designer can constrain the allowable coverage and use the motion algorithms to achieve different QoS improvements.

Table 3. Different topological characteristics and corresponding improvements in location determination using goal-directed motion (# nodes = 30)

Coverage	Diameter	NC.	ξ (%)	Improvement (%)
Random Way Point		5	22	NA
55	4	16	7	68.1
62	6	15	8	63.6
70	6	13	9	59.1
80	6	11	12	45.5
80	8	9.5	13	41

6. Conclusions

The paper presented a simulation based study of topological characteristics of a mobile sensor network. The study investigated the individual and combined effects of connectivity, coverage, and diameter on the number of sensor nodes that need to be deployed and concluded that it is coverage that dictates the requirement for the network under study. Next, permanent and transient errors were introduced. The study brought out the effect of varying the MTTF and the ratio of permanent to transient failures and concluded that small increases in permanent failure rates have a large effect on the network characteristics. The paper also presented the effect of topological characteristics on the QoS of a location determination application. The error in location estimation was reduced by up to 68% by the mobility algorithms compared to a random waypoint model.

For future work, the effect of the variation of transmission range on the parameters, and time varying and heterogeneous transmission ranges need to be investigated. It would be interesting to study the sensitivity of the parameters of interest to failures in the links. An investigation of what network characteristics are required for supporting different classes of applications (location determination, soft real-time, etc.) would make an important contribution to the adoption of sensor networks. Since sensor networks are severely energy constrained, it would be important to evaluate the energy

cost of the mobility algorithms presented here and evaluate the conditions under which they will be feasible.

7. References

- [1] J. Moy, OSPF Version 2, *RFC 1247*, July 1991.
- [2] C. Hedrick, Routing Information Protocol, *RFC 1058*, June 1988.
- [3] R. C. Shah, J. M. Rabaey, "Energy aware routing for low energy ad hoc sensor networks", *Wireless Communications and Networking Conference (WCNC)*, 2002.
- [4] P. Santi, D. M. Blough, "An evaluation of connectivity in mobile wireless ad hoc networks", *IEEE Dependable Systems and Networks Conference (DSN)*, 2002, pp.89-98.
- [5] Chris Savarese, Jan Rabaey, Koen Langendoen, "Robust Positioning Algorithms for Distributed Ad-Hoc Wireless Sensor Networks", *USENIX Technical Annual Conference*, June 2002.
- [6] J. Beutel, "Geolocation in a Pico Radio Environment", *Master's thesis*, ETH Zurich, December 1999.
- [7] Paolo Santi, Douglas M. Blough, Feodor Vainstein, "A probabilistic analysis for the range assignment problem in ad hoc networks", *Mobihoc 2001*, pp.212-220.
- [8] Christian Bettstetter, "On the minimum node degree and connectivity of a wireless multihop network", *ACM Mobihoc*, 2002, pp.80-91.
- [9] Chris Savarese, "Robust Positioning Algorithms for Distributed Ad-Hoc Wireless Sensor Networks", 2002 *M.S. thesis (advisor Jan Rabaey)*, Berkeley Wireless Research Center.
- [10] S. Bagchi, S. Cabuk, N. Malhotra, "Modeling and Evaluation of Topological and Application Characteristics on Mobile Wireless Ad Hoc Networks". *Technical Report*, Dept. of ECE, Purdue University. Available at: <http://www.ece.purdue.edu/~sbagchi>
- [11] P. Gupta, P.R. Kumar, "The capacity of wireless network", *IEEE Transactions on Information Theory*, vol. IT-46, no. 2, pp. 388-404, March 2000.
- [12] S. Shakkottai, R. Srikant, N. Shroff, "Unreliable Sensor Grids: Coverage, Connectivity and Diameter", *INFOCOM 2003*, pp.1073-1083.
- [13] Yizong Cheng, "Mean shift, mode seeking, and clustering", *IEEE Transactions on Pattern Analysis and Machine Intelligence*, Volume: 17 Issue: 8, Aug. 1995, pp. 790-799.
- [14] Christian Bettstetter, Hannes Hartenstein, and Xavier Pérez-Costa, "Stochastic Properties of the Random Waypoint Mobility Model", *ACM/Kluwer Wireless Networks, Special Issue on Modeling and Analysis of Mobile Networks*, accepted Mar 2003, To appear 2004.